

DESIGN OF AN EDUCATIONAL MINI DRONE SPECIFICALLY ENGINEERED FOR 3D PRINTING WITH OPTIMAL STRUCTURAL STRENGTH

¹Syafrizal Nofriade, ^{*2}Rudi Kurniawan Arief, ³Jana Hafiza, ⁴Yuni Vadila

^{1,2,3}Mechanical Engineering, Faculty of Engineering, Muhammadiyah University of West Sumatra
Padang, Indonesia

⁴Mechanical Engineering, Faculty of Engineering, Padang State University
Padang, Indonesia

Author's email:

¹syafrizalnofriade9@gmail.com; ^{2*}rudikarief@umsb.ac.id; ³janahafizaumsb@gmail.com

⁴yunifadilabkt@gmail.com

*Corresponding author: rudikarief@umsb.ac.id

Abstract. *The development of mini drones as educational platforms in engineering disciplines requires a frame design that is lightweight, manufacturable, and structurally reliable. Additive manufacturing using Fused Deposition Modeling (FDM) provides high design flexibility and cost efficiency; However, the mechanical performance of 3D-printed structures is strongly influenced by their geometric configuration. Therefore, a dedicated design approach is required to ensure sufficient structural strength for educational mini drone frames fabricated using FDM. This study aims to design and evaluate a 3D-printed educational mini drone frame made of polyethylene terephthalate glycol (PETG) with optimized structural performance. The research methodology includes computer-aided design (CAD)-based geometric modeling, analytical calculations using classical mechanics of materials, static load testing, and numerical simulation using Finite Element Analysis (FEA) in SolidWorks Simulation. The structural response was evaluated in terms of displacement, Von Mises stress, strain, and factor of safety. The simulation results indicate a maximum displacement of 1.31 mm, a maximum Von Mises stress of 49,417 MPa, and a maximum equivalent strain of approximately 0.0235 (2.35%). The minimum factor of safety was found to be 1.00, while the maximum value reached 5.34. A comparison between analytical and FEA results shows consistent structural response trends, although numerical differences occur due to three-dimensional geometric effects and local stress concentrations. Overall, the proposed mini drone frame is structurally feasible for educational applications and provides a reliable basis for further design optimization, particularly in the central body region.*

Keywords: *Educational Mini Drones; Factor of Safety; Finite Element Analysis; 3D Printing; PETG; Structural Analysis.*

1. INTRODUCTION

The development of mini-scale Unmanned Aerial Vehicle (UAV) technology shows a significant increase in its use as a learning medium in the field of engineering. (R. et al., 2025) Educational mini drones are used as a hands-on learning tool that integrates mechanical design, aerodynamic principles, and the application of modern manufacturing technology. In this context, drone frame design is crucial because it serves as the primary structure supporting all components and operational loads. (Usma et al., 2024).

Additive manufacturing technology through 3D printing, especially the Fused Deposition Modeling (FDM) method, is widely applied in the manufacture of mini drone frames because it offers design flexibility, time efficiency, and relatively low production costs. (Vadila, nd) However, the mechanical characteristics of 3D-printed components are heavily influenced by geometric design and printing process parameters, such as infill pattern, infill density, layer orientation, and wall thickness. Inappropriate design and printing parameter selection can potentially reduce the structural strength and reliability of the drone frame during use.

Previous research generally discusses the influence of 3D printing parameters on the mechanical properties of materials separately or evaluates drone performance from the aspects of aerodynamics and flight stability. (Jadhav & Jadhav, 2022) Several studies have examined the

relationship between infill density and the mechanical strength of 3D-printed specimens, but studies that integrate mini drone frame design with structural strength optimization specifically tailored for 3D printing technology are still limited, especially in the context of educational mini drones. This indicates a research gap related to the integration of structural design and printing parameters in producing optimal mini drone frames.(3D Printing, etc.).

Based on these problems, this research aims to design an educational mini drone that is specifically designed for 3D printing with optimal structural strength.(Parupelli & Desai, 2019)This research is expected to produce a mini drone frame design that is efficient, structurally reliable, and suitable for learning needs, as well as provide academic contributions in the development of additive manufacturing-based product design in the field of engineering.

2. LITERATURE REVIEW

2.1 Educational Mini Drone and Structural Design

Educational mini drones are a form of technology-based learning tool that is used to support engineering learning in a contextual and applicable manner.(Sarkar & Johnson, 2022)The use of drones in engineering education enables the integration of mechanical design, aerodynamics, propulsion systems, and manufacturing concepts into a single, integrated learning platform. Therefore, the design of educational mini drones requires not only functional requirements but also safety, ease of replication, and adequate structural reliability.

The drone frame is the primary structural element that supports all components and operational loads. Several studies have confirmed that structural failures in drone frames are generally caused by suboptimal geometric design for static and dynamic load distribution. In the context of mini drones, structural optimization becomes even more critical because mass and dimension limitations significantly impact flight performance.(K. Isabella Rani, 2025).

Modern structural design approaches often adopt numerical analysis, particularly Finite Element Analysis (FEA), to evaluate stress distribution and deformation in drone frames prior to manufacturing. This method allows for the identification of critical structural points and the evaluation of the effectiveness of geometry modifications without significantly increasing mass. However, most research still focuses on structural analysis without considering the limitations and specific characteristics of the manufacturing technology used.

2.2 3D Printing and the Effect of Parameters on Mechanical Strength

3D printing-based additive manufacturing technology, particularly the Fused Deposition Modeling (FDM) method, is widely used in the manufacture of mini drone components due to its design flexibility and cost-effectiveness. However, 3D-printed components are anisotropic, so their mechanical strength is highly influenced by the printing process parameters.(Malik et al., 2025).

Several studies have shown that molding parameters such as infill density, infill pattern, layer orientation, and wall thickness have a significant influence on tensile strength, flexural strength, and impact resistance. Nonlinear infill patterns, such as gyroid and honeycomb, are reported to produce a more even stress distribution than conventional linear patterns. However, increasing mechanical strength is often accompanied by an increase in mass and molding time, so an optimization approach that considers both aspects simultaneously is needed.

Several recent studies have examined the relationship between geometric design and 3D printing parameters, but these have generally been conducted on standardized test specimens, rather than functional structures such as drone frames. Consequently, the application of these research findings to educational mini-drone design still faces contextual limitations.(Mukherjee, 2021).

2.3 Integration of Structural Design with Additive Manufacturing

The integration of structural design and additive manufacturing processes is a crucial approach in the development of modern engineered products. Design for Additive

Manufacturing (DfAM) emphasizes that component design must be adapted from the outset to the characteristics of the 3D printing process, including geometric constraints, printing direction, and anisotropic mechanical properties of the material. This approach aims to improve structural performance while reducing manufacturing failures. (St et al., 2025).

Several studies have shown that structurally optimized designs that do not take into account the limitations of 3D printing can result in components that are difficult to print or have low mechanical quality. (Supriyati & Widya, 2025) In the context of mini drone frames, the integration of structural design with additive manufacturing becomes crucial because the structure must be able to withstand dynamic loads, vibrations, and impact forces, while still being able to be printed efficiently without requiring excessive support structures.

3. RESEARCH METHODS

This study used an engineering design-based experimental approach combined with analytical structural analysis and numerical simulation to evaluate the performance of a 3D-printed mini drone frame. The study was conducted from November 2025 to January 2026 at the Computer Laboratory of the University of Muhammadiyah West Sumatra. The research flow used in this study is shown in Figure 1.

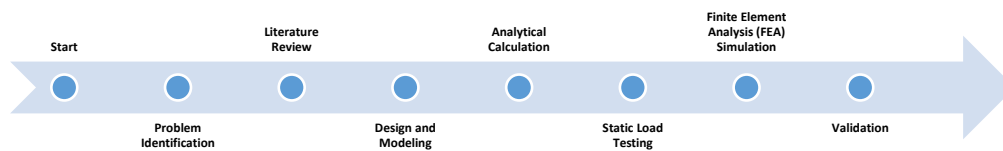


Figure 1. Flowchart

3.1 Geometric Design

The frame was designed using CAD software with a truss-braced hollow arm structure to improve strength-to-weight ratio. Fillets were applied at the arm and midbody joints to reduce stress concentrations. The same 3D model was used for analytical calculations, testing, and numerical simulations to maintain geometric consistency.

3.2 Analytical Modeling and Calculations

To obtain an initial prediction of the structural response, each arm of the frame is modeled as a hollow-section cantilever beam with a concentrated load at the arm end. The main structural parameters are calculated using the following mechanics of materials equations.

Moment of inertia of cross section:

$$I = \frac{\pi}{4}(R^4 - r^4) \quad \dots(1)$$

Maximum bending stress:

$$\sigma_{max} = \frac{M_{max} \cdot c}{I} \quad \text{with} \quad M_{max} = F \cdot L \quad \dots(2) \text{ and } (3)$$

Maximum deflection:

$$\delta_{max} = \frac{FL^3}{3EI} \quad \dots(4)$$

Safety factors:

$$FOS = \frac{\sigma_y}{\sigma_{max}} \quad \dots(5)$$

The results of analytical calculations are used as an initial reference to evaluate the feasibility

of the design before testing and simulation are carried out.

3.3 Static Test

Experimental testing was conducted using static load tests, in which the center body of the frame was clamped as a support and the load was gradually applied to the ends of the arms. The maximum deflection was measured using precision measuring instruments and used as validation data against the analytical results.

3.4 Finite Element Analysis (FEA) Simulation

Numerical simulations were performed using SolidWorks Simulation. The CAD model was subjected to boundary conditions representing midbody restraints and loading equivalent to static tests. The analysis included displacement, Von Mises stress, and factor of safety. Meshing was performed using adaptive tetrahedral elements.

3.5 Data Analysis and Validation

The results of analytical calculations, static tests, and FEA simulations were compared quantitatively. The level of agreement between the methods was evaluated based on the similarity of structural response trends and the magnitude of numerical deviations. The design was declared valid if the maximum stress was below the yield stress of PETG, the deflection was within acceptable limits, and the safety factor was greater than one.

4. RESULTS AND DISCUSSION

4.1 Results of Mini Drone Frame Geometry Design

The geometric design results of the mini drone frame are shown in **Figure 2**, which shows a quad-X configuration frame structure with four hollow arms and truss reinforcement. The effective length of each frame arm is 48.3 mm, with an average wall thickness of 2 mm. These dimensions are designed to increase the moment of inertia of the cross-section without significantly increasing the mass.

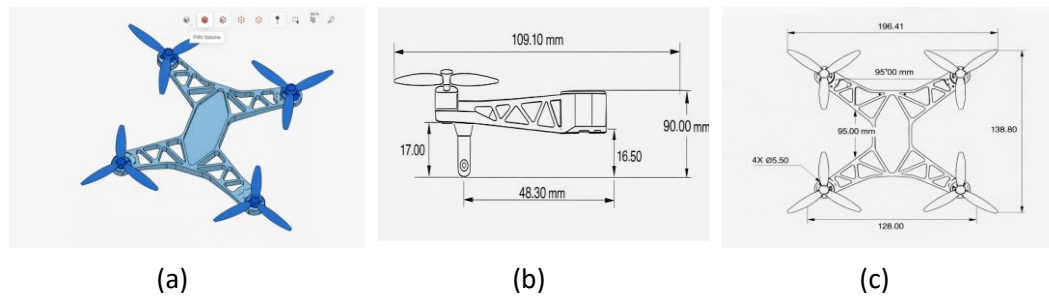


Figure 2. Mini Drone Frame Geometry

The moment of inertia of the hollow arm cross-section is calculated using the equation:

$$I = \frac{\pi}{4} (R^4 - r^4)$$

With the outer radius and inner radius, the moment of inertia is: $R = 6\text{ mm}$ and $r = 4\text{ mm}$

$$I = 816,81\text{ mm}^4$$

This value is the main parameter in calculating bending stress and deflection at the analytical stage.

4.2 Displacement Analysis Results

The results of the Finite Element Analysis simulation for displacement are shown in Figure 3.

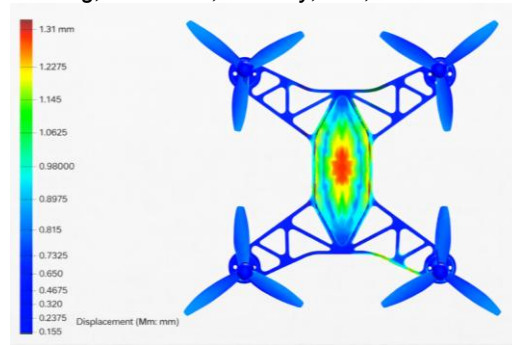


Figure 3. Displacement

Based on the color legend in the simulation results, the following displacement values are obtained:

1. maximum displacement: 1.31 mm,
2. minimum displacement: 0.155 mm.

The maximum displacement occurs in the center body of the frame, while the arm and motor mount areas exhibit much smaller displacements. This pattern indicates that the center body experiences accumulated deformation due to global load distribution.

Analytically, the maximum deflection is calculated using the cantilever beam equation:

$$\begin{aligned} \delta_{max} &= \frac{FL^3}{3EI} \\ \delta_{max} &= \frac{43,4 \times (0,04830)^3}{3 \times 2.1 \times 10^9 \times 8,17 \times 10^{-10}} \\ \delta_{max} &= \frac{43,4 \times 1,13 \times 10^{-4}}{5,14} \\ \delta_{max} &= 9,5 \times 10^{-4} \\ &= 0,95 \text{ mm} \end{aligned}$$

The theoretical deflection values are in the sub-millimeter range, approaching 1 mm. The difference with the FEA results of 1.31 mm is due to the effects of three-dimensional deformations in the midbody that are not accommodated in the one-dimensional beam model.

However, the maximum displacement value of 1.31 mm is still within the elastic limit and does not have the potential to cause structural disturbances to the frame.

4.3 Results of Von Mises Stress Analysis

The Von Mises stress distribution resulting from the FEA simulation is shown in Figure 4.

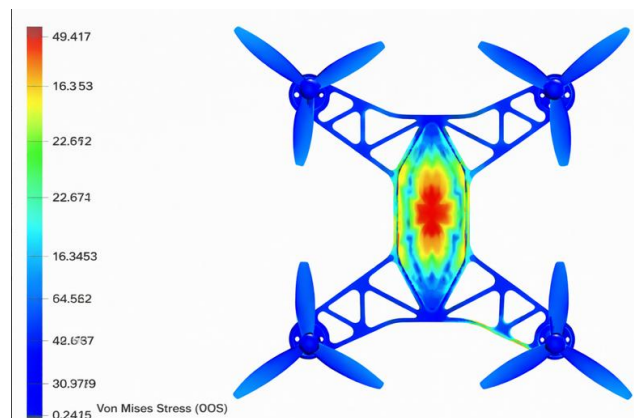


Figure 4. Von Mises stress

Based on the color legend, the voltage values are as follows:

1. maximum Von Mises stress : 49.417 MPa,
2. minimum voltage : 0.2415 MPa.

The maximum stress is localized in the center of the frame, specifically where the arms meet the main body. This location represents a region of cross-sectional changes and force flow paths, making it theoretically prone to stress concentration.

Analytically, the maximum bending stress is calculated using:

$$\sigma_{max} = \frac{M_{max}.c}{I}$$

with

$$M_{max} = F.L$$

$$M_{max} = 43,4 N \times 0,04830$$

$$M_{max} = 2,10 N$$

So:

$$\sigma_{max} = \frac{2,10 \times 0,006}{8,17 \times 10^{-10}}$$

$$\sigma_{max} = 15,4 \times 10^6 Pa$$

$$= 15,4 MPa$$

The analytical approach yields lower stress values because it assumes the arms are ideal one-dimensional beams. The FEA simulation yields higher values because it considers the effects of complex geometry, fillets, and inter-arm interactions through the midbody.

4.4 Results of Safety Factor Analysis



Figure 5. Factor of Safety

The distribution of safety factors resulting from the FEA simulation is shown in Figure 5. Based on the simulation legend, the following is obtained:

1. minimum safety factor: 1.00,
2. maximum safety factor: 5.34.

The minimum FOS value is in the same area as the maximum Von Mises stress, namely in the center of the frame. Meanwhile, the outer arm and motor mount areas have much higher FOS values.

Theoretically, the safety factor is calculated using:

$$FOS = \frac{\sigma_y}{\sigma_{max}}$$

$$100 = \frac{\sigma_y}{49,417 MPa}$$

$$\sigma_y = 1,00 \times 49,417 MPa$$

$$\sigma_y = 49,417 MPa$$

With a maximum Von Mises stress of 49.417 MPa, the minimum FOS value of 1.00 indicates

that the structure is right at the elastic safety limit of PETG material. This condition is still acceptable for educational applications with controlled loads, but indicates that the midbody is a critical zone with potential for design optimization.

4.5 Strain Analysis Results and Calculations (PETG Material)

The results of the strain distribution simulation on the mini drone frame are shown in Figure 6.

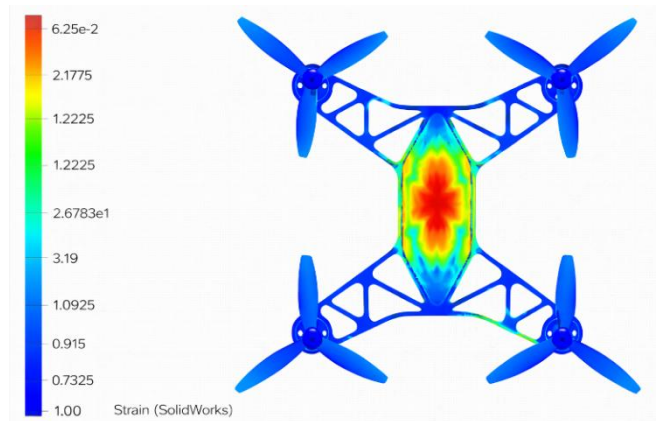


Figure 6. Strain

$$\varepsilon = \frac{\sigma}{E}$$

Since the simulation results used are Von Mises equivalent stress, the equivalent strain estimate (approximation) can be calculated as:

$$\begin{aligned}\varepsilon_{eq.max} &= \frac{\sigma_{VM}}{E} \\ \varepsilon_{eq.max} &= \frac{49,417 \times 10^6}{2,1 \times 10^9} \\ \varepsilon_{eq.max} &= 2,353 \times 10^{-2} \\ \varepsilon_{eq.max} &= 0,0233 \text{ atau } 2,35\%\end{aligned}$$

As a geometric comparison, the average strain can also be estimated from the global deformation:

$$\begin{aligned}\varepsilon_{geo} &= \frac{\Delta L}{L} = \frac{\delta_{max}}{L} \\ &= \frac{1,31}{48,30} \\ &= 0,0271 \text{ (2,71\%)}\end{aligned}$$

Both approaches yield strains on the order of 2–3%, indicating internal physical consistency: relatively high displacements in the midbody are indeed accompanied by increased strain and stress in that zone. The differences between the estimates arise from:

1. $\varepsilon = \sigma/E$ represents equivalent local strain (material-based),
2. while representing the global deformation of the structure (geometry-based). δ/L

Thus, strain becomes a link that strengthens the consistency between stress and displacement results.

4.6 Discussion of the Relationship between Analytical Results and FEA

results of analytical calculations and Finite Element Analysis (FEA) simulations demonstrates a consistent relationship in describing the structural response of a PETG mini drone frame. The analytical approach, which models the frame arms as hollow-section cantilever beams, provides

an initial estimate of the structure's flexural behavior. Meanwhile, FEA captures a more realistic three-dimensional response, including the effects of complex geometry, connections, and global load distribution.

The Von Mises stress distribution from the FEA results shows a maximum value of 49.417 MPa concentrated at the center of the frame. This location is consistent with the analytical prediction that the area where the arm and body meet will experience the greatest bending moments and internal forces. The difference in numerical values between analytical and FEA stresses is primarily due to the limitations of the one-dimensional beam model, which is unable to represent the local stress concentrations and multiaxial stress conditions analyzed by FEA.

The FEA displacement results show a maximum deformation of 1.31 mm, with a minimum deformation of approximately 0.155 mm. This deformation pattern aligns with the analytical results, which show that deformation increases with increasing bending moment and effective arm length. The higher FEA displacement values reflect the contribution of global deformation to the midbody, which is not fully captured by the single-beam analytical calculations.

The consistency between stress and displacement is also reflected in the strain results. Based on the linear-elastic relationship, the maximum equivalent strain is estimated to be 0.0235 (2.35%) of the ratio of the maximum Von Mises stress to the elastic modulus of PETG. This estimate is comparable to the global deformation-based geometric strain, which is approximately 0.0271 (2.71%), indicating that the increase in global deformation is directly correlated with the increase in material strain in the critical zone.

The relationship between stress and safety factor also shows strong consistency. The minimum safety factor from the FEA results is 1.00, which occurs at the location of maximum stress, while the maximum safety factor reaches 5.34 in the area of low stress. These results are consistent with the definition of safety factor as the ratio between the yield stress of a material and the working stress, so that a decrease in the safety factor is directly related to an increase in the Von Mises stress.

Overall, the correlation between analytical and FEA results demonstrates a complementary approach. Analytical calculations serve as a simple and conservative initial prediction tool, while FEA provides a thorough evaluation of the most critical structural conditions. Consistent trends among stress, displacement, strain, and safety factors indicate that the proposed mini drone frame design is elastic and acceptable for educational applications, although the center body is identified as the area with the greatest potential for further optimization.

CONCLUSION

Based on the design results, analytical calculations, and Finite Element Analysis (FEA) simulations of the PETG mini drone frame, it can be concluded that the proposed design has consistent structural performance and can be scientifically justified. The frame geometry with a quad-X configuration and a hollow arm structure with truss reinforcement is able to distribute the load effectively, so that deformation and stress do not accumulate at the end of the arm or motor mount, but are concentrated in the center body of the frame.

The FEA simulation results show that the frame experiences a maximum Von Mises stress of 49.417 MPa, a maximum displacement of 1.31 mm, and a maximum equivalent strain of approximately 0.0235 (2.35%). The minimum safety factor obtained is 1.00, indicating that the structure is within the elastic safety limit of the PETG material used in the simulation. Meanwhile, most areas of the frame have a higher safety factor, with a maximum value reaching 5.34, indicating an uneven but controlled stress distribution.

A comparison of the analytical and FEA results indicates a good agreement between the structural response trends, particularly in identifying the critical zone locations and the physical relationships between stress, strain, displacement, and safety factors. The differences in numerical values between the two approaches are due to idealization in the analytical

calculations, which model the structure as a one-dimensional beam, while FEA captures three-dimensional effects, local stress concentrations, and global midbody deformations. Nevertheless, the analytical results still serve as valid initial predictions and provide a basis for verifying the numerical simulation results.

Overall, the designed PETG mini drone frame was found to be structurally feasible for educational applications, with the midbody being the most critical area and potentially subject to further optimization. These findings confirm that integrating geometric design, analytical calculations, and FEA simulations is an effective approach in developing lightweight, functional, and safe 3D-printed mini drone frames.

REFERENCES

- 3D Printing*. (ND). [Dataset]. <https://Doi.Org/10.1036/1097-8542.694300>
- Jadhav, A., & Jadhav, V. S. (2022). A Review On 3D Printing: An Additive Manufacturing Technology. *Materials Today: Proceedings*, 62, 2094–2099. <https://Doi.Org/10.1016/J.Matpr.2022.02.558>
- K. Isabella Rani. (2025). Magnetic-Powered Mini Drones For Smart IOT-Driven Agricultural Solutions. *International Journal Of Advanced Research And Interdisciplinary Scientific Endeavors*, 2(4), 550–560. <https://Doi.Org/10.61359/11.2206-2517>
- Malik, A., Parihar, V., & Sharma, U. (2025). The Investigation On Mechanical Properties And Failure Mechanism Identification Of A 3D Printed Object. *2025 3rd International Conference On Disruptive Technologies (ICDT)*, 30–35. <https://Doi.Org/10.1109/ICDT63985.2025.10986695>
- Mukherjee, T. (2021). Special Issue: The Science And Technology Of 3D Printing. *Materials*, 14(21), 6261. <https://Doi.Org/10.3390/Ma14216261>
- Parupelli, S. K., & Desai, S. (2019). A Comprehensive Review Of Additive Manufacturing (3D Printing): Processes, Applications And Future Potential. *American Journal Of Applied Sciences*, 16(8), 244–272. <https://Doi.Org/10.3844/Ajassp.2019.244.272>
- Mukt Hukumar (2025). Face Tracking Mini Drone. *Journal Of Information Technology And Digital World*, 7(2), 189–199. <https://Doi.Org/10.36548/Jitdw.2025.2.008>
- Sarkar, S., & Johnson, N. P. (2022). A Deep-Learning, Vision-Based Framework For Testing Swarm Algorithms Using Inexpensive Mini Drones. In PL Muench, HG Nguyen, & BK Skibba (Eds.), *Unmanned Systems Technology XXIV* (P. 12). SPIE. <https://Doi.Org/10.1117/12.2618137>
- St, BH, Murtiadi, S., & Suryani, F. (2025). Integration of Design Model and Implementation Strategy of Steel Construction in New Factory Industrial Building in Karawang International Industrial City: Integration of Design Model and Implementation Strategy of Steel Construction in New Factory Industrial Building in Karawang International Industrial City. *Sainstech: Journal of Research and Assessment of Science and Technology*, 35(4), 12–23. <https://Doi.Org/10.37277/Stch.V35i4.2439>
- Supriyati, S., & Widya, AR (2025). Integration of Theory and Practice of Product Design and Development Processes (In the Automotive Component Manufacturing Industry). *Journal of Multidisciplinary Science*, 4(4), 2548–2560. <https://Doi.Org/10.38035/Jim.V4i4.1343>
- Usma, UIW, Setiawan, F., Sofyan, E., & Imama. (2024). The Effect of Manufacturing Thickness of 3D Printing Mini Drone Frames with Stress, Displacement, and Safety of Factor Simulations Using Solidworks Software. *Teknika Sttkd: Journal of Engineering, Electronics, Engines*, 9(2), 359–369. <https://Doi.Org/10.56521/Teknika.V9i2.973>
- Vadila, Y. (ND). Design And Fabrication Of Fused Deposition Modeling 3D Printer For Early-Age Students Using Quality Function Deployment Method.